

# The X–ray transient XTE J1859+226 in Outburst & Quiescence

C. Zurita<sup>1\*</sup>, C. Sánchez–Fernández<sup>2</sup>, J. Casares<sup>1</sup>, P.A. Charles<sup>3</sup>, T.M. Abbott<sup>4</sup>,  
P. Hakala<sup>5</sup>, P. Rodríguez–Gil<sup>1</sup>, S. Bernabei<sup>6</sup>, A. Piccioni<sup>7</sup>, A. Guarnieri<sup>7</sup>, C. Bartolini<sup>7</sup>,  
N. Masetti<sup>8</sup>, T. Shahbaz<sup>1</sup>, A. Castro–Tirado<sup>9</sup>

<sup>1</sup>*Instituto de Astrofísica de Canarias, 38200 La Laguna, Tenerife, Spain*

<sup>2</sup>*Laboratorio de Astrofísica Espacial y Física Fundamental (LAEFF-INTA), 28080 Madrid, Spain*

<sup>3</sup>*Department of Physics and Astronomy, University of Southampton, Southampton, SO17 1BJ, UK*

<sup>4</sup>*Nordic Optical Telescope, 38700 Santa Cruz de La Palma, Spain.*

<sup>5</sup>*Observatory and Astrophysics Laboratory, FIN-00014 University of Helsinki, Finland*

<sup>6</sup>*Osservatorio Astronomico di Bologna, Via Ranzani 1 Bologna, Italy*

<sup>7</sup>*Dipartimento di Astronomia, Università di Bologna, Via Ranzani 1 Bologna, Italy*

<sup>8</sup>*Istituto Tecnologie e Studio Radiazioni Extraterrestri, CNR, Via Gobetti 101, 40129 Bologna, Italy*

<sup>9</sup>*Instituto de Astrofísica de Andalucía, 18080 Granada, Spain*

5 October 2021

## ABSTRACT

We present optical photometry and spectroscopy of the X–ray transient XTE J1859+226, obtained during outburst and its subsequent decay to quiescence. Both the X–ray and optical properties are very similar to those of well–studied black hole soft X–ray transients. We have detected 3 minioutbursts, when XTE J1859+226 was approaching quiescence, as has been previously detected in the Soft X–Ray Transients GRO J0422+32 and GRS 1009–45. By 24 Aug 2000 the system had reached quiescence with  $R=22.48\pm 0.07$ . The estimated distance to the source is  $\sim 11$  kpc. Photometry taken during quiescence shows a sinusoidal modulation with a peak to peak amplitude of about 0.4 mag. A period analysis suggests that periods from 0.28 to 0.47 days are equally possible at the 68% confidence level. The amplitude of the quiescent light curve and the relatively low ratio of X–ray to optical flux, indicates that the binary inclination should be high. The measured colours during the outburst allows us to obtain the basic properties of the disc, which agrees well with irradiated disc model predictions.

**Key words:** black hole physics–binaries:close–stars: individual: XTE J1859+226–X–rays:stars

## 1 INTRODUCTION

Soft X-ray transients (SXTs) are a subclass of low-mass X-ray binaries (LMXBs) that are characterized by episodic X-ray outbursts (usually lasting for several months), when the X-ray luminosities can increase by as much as a factor of  $10^7$  (van Paradijs & McClintock 1995). The observed optical flux is generated by X-ray reprocessing in the accretion disc and the companion star. These outbursts recur on a timescale of decades, but in the interim the SXTs are in a state of quiescence and the optical emission is dominated by the radiation of the faint companion star. This offers the

best opportunity to analyze the properties of this star and obtain dynamical information which eventually enables us to constrain the nature of the compact object. There are currently 17 SXTs with identified optical counterparts, with 13 dynamically studied black-holes and 4 confirmed neutron stars.

The X–ray transient J1859+226, was discovered by the All–Sky Monitor (*ASM*) on board the Rossi X–Ray Timing Explorer (*RXTE*) on 1999 October 9 (Wood et al. 1999) and subsequently identified with a  $R=15.1$  variable star (Garnavich & Quinn 2000). Spectra during outburst showed typical LMXB features (Wagner et al. 1999). The dereddened optical energy distribution was represented by a steep blue power law flattening in the ultraviolet which suggested a bi-

\* e-mail: czurita@ll.iac.es

nary period  $\leq 1$  day. Although no persistent coherent modulation was detected, a low amplitude (1 per cent modulation) with a period of 22–23 min was seen (Hynes et al. 1999). Subsequent photometry revealed other modulations with periods of 0.2806 days (Uemura et al. 1999) and 0.3813 days (Garnavich et al. 1999), but none of them could be confirmed. Nine months after the outburst, but still not in quiescence, a new 0.78 day period was reported (McClintock et al. 2000). Light curves folded on this period showed a 0.2 mag primary minimum (interpreted as a partial eclipse of the accretion disc by the secondary star), and a shallow secondary minimum (explained as an eclipse of the star by the disc).

Here we present our extensive optical photometry of the entire outburst, the subsequent minioutburst and the first quiescent photometry. Some of these results have received preliminary announcements in Sánchez-Fernández et al. 2000, Zurita et al. 2000 and Charles et al. 2000.

## 2 OBSERVATIONS AND DATA REDUCTION

### 2.1 Photometry

Our long-term monitoring campaign was carried out during the period Oct. 1999– Sep. 2000 with the 80 cm IAC80 and 1m Optical Ground Station (OGS) at the Observatorio del Teide; 1m JKT, 2.5m NOT, 3.5m TNG and 4.5m WHT at the Observatorio del Roque de los Muchachos; 1.5m OAN and 2.2m CAHA at Observatorio de Calar Alto and 1.52m telescope at Loiano. We obtained CCD images mainly in *R*-band but also some *B*, *V*, *I* colours. Integration times ranged from 30 s to 40 min, depending on the telescope, atmospheric conditions and the star brightness. The observing log with full details is given in Table 1. All the images were de-biased and flat-fielded in the standard way using IRAF.

We applied aperture photometry to our object and several nearby comparison stars within the field of view, using IRAF. We selected several comparison stars which were checked for variability during each night, and over the entire data set. Calibration of the data was performed using 17 standard stars from several fields (Landolt 2000), to construct a colour dependent calibration. Frames taken during quiescence with the WHT and good seeing conditions, revealed the presence of a faint nearby star  $\sim 1.4$  arcsec North of the target (see Figure 1). We applied psf photometry using the IRAF routine DAOPHOT (Stetson 1987). We found a magnitude of  $R=23.05\pm 0.04$  for the contaminating star. We also recalibrated a set of 5 faint comparison stars from the previous calibrated set, using these images (see Table 3).

### 2.2 Spectroscopy

Spectroscopic observations of XTE J1859+226 were carried out at primary outburst and during one of the minioutbursts. The observing log for these observations is presented in Table 2. The first series of optical spectra of the source were obtained on Oct. 28–29, 1999, when 31 exposures were taken in the Isaac Newton Telescope (INT) at the Observatorio del Roque de los Muchachos, using the EEV10 camera

**Table 1.** Log of photometric observations (Oct 1999 –May 2000)

<i>Date</i>	<i>HJD</i> (*)	<i>Exp/Filter</i>	<i>Telescope</i>
<i>Oct15</i>	7	1xR	0.8m IAC80
<i>Oct17</i>	9	10xI,21xR,2xV,2xB	0.8m IAC80
<i>Oct18</i>	10	111xR,1xV,1xB	0.8m IAC80
<i>Oct19</i>	11	106xR,1xV,1xB	0.8m IAC80
<i>Oct20</i>	12	1xI,110xR,1xV,1xB	0.8m IAC80
<i>Oct21</i>	13	2xR,1xV,1xB	0.8m IAC80
<i>Oct23</i>	15	1xR	0.8m IAC80
<i>Oct28</i>	20	3xR	0.8m IAC80
<i>Oct29</i>	21	1xI,111xR,1xV,1xB	0.8m IAC80
<i>Nov07</i>	29	128xR	1.5m OAN
<i>Nov27</i>	50	30xR,1xV,1xB	0.8m IAC80
<i>Nov28</i>	51	40xR,1xV,1xB	0.8m IAC80
<i>Dic10</i>	63	2xR	0.8m IAC80
<i>Dic12</i>	65	4xR,1xV,1xB	0.8m IAC80
<i>Dic16</i>	69	1xR	0.8m IAC80
<i>Jan03</i>	87	3xR	2.2m CAHA
<i>Jan04</i>	88	3xV	2.2m CAHA
<i>Jan05</i>	89	1xB	2.2m CAHA
<i>Feb01</i>	116	1xR	0.8m IAC80
<i>Feb04</i>	119	1xI,1xR,1xV,1xB	1m OGS
<i>Feb05</i>	120	1xI,1xR,1xV,1xB	1m OGS
<i>Feb06</i>	121	1xI,2xR,1xV,1xB	1m OGS
<i>Feb07</i>	122	1xI,1xR,1xV,1xB	1m OGS
<i>Feb08</i>	123	1xI,1xR,1xV,1xB	1m OGS
<i>Feb09</i>	124	1xI,1xR,1xV,1xB	1m OGS
<i>Feb10</i>	125	1xI,1xR,1xV,1xB	1m OGS
<i>Feb11</i>	126	2xI,2xR,2xV,2xB	1m OGS
<i>Feb12</i>	127	1xI,2xR,1xV,1xB	1m OGS
<i>Feb13</i>	128	2xI,2xR,1xV,1xB	1m OGS
<i>Feb14</i>	129	3xI,2xR,1xV,1xB	1m OGS
<i>Feb15</i>	130	2xI,1xR,2xV,2xB	1m OGS
<i>Feb20</i>	135	1xR	1m OGS
<i>Feb27</i>	142	1xR	0.8m IAC80
<i>Mar03</i>	145	1xR	0.8m IAC80
<i>Mar16</i>	160	1xV,1xR	0.8m IAC80
<i>Mar23</i>	167	1xV,1xR	0.8m IAC80
<i>Mar24</i>	167-8	10xR	Lowell
		1xV,1xR	0.8m IAC80
<i>Mar25</i>	168	1xR	Lowell
<i>Mar27</i>	170-1	30xR	Lowell
<i>Apr03</i>	178	1xV,1xR	0.8m IAC80
<i>Apr04</i>	179	1xV,1xR	0.8m IAC80
<i>Apr05</i>	180	1xR	0.8m IAC80
<i>Apr10</i>	185	1xV,1xR	0.8m IAC80
<i>Apr16</i>	191	1xR	0.8m IAC80
<i>Apr25</i>	200	1xV,1xR	0.8m IAC80
<i>Apr28</i>	203	2xR	0.8m IAC80
<i>May16</i>	221	2xR	0.8m IAC80
<i>May17</i>	222	1xR	0.8m IAC80
<i>May23</i>	228	2xR	1.52 Loiano
<i>May24</i>	229	2xR	1.52 Loiano
<i>May25</i>	230	2xR	0.8m IAC80
		3xR	1.52 Loiano

\*HJD–2451460

**Table 1** – *continued* Log of photometric observations (Jun–Nov 2000)

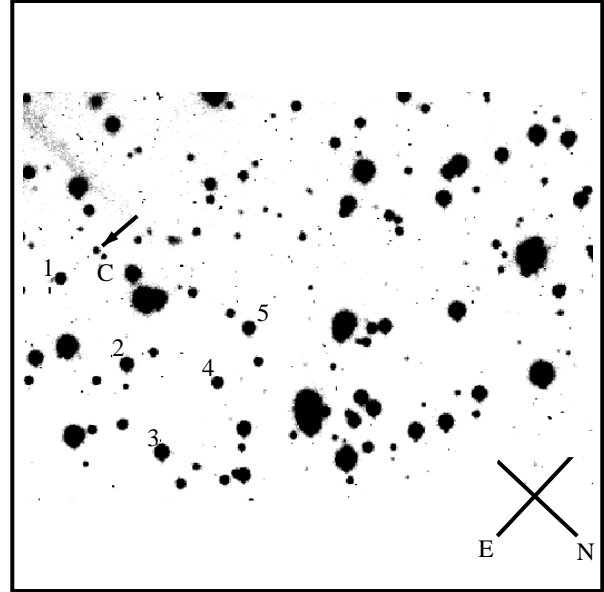
Date	HJD(*)	Exp/Filter	Telescope
Jun01	237	37xR	1m OGS
Jun03	239	34xR	1m OGS
Jun04	240	64xR	1m OGS
Jun06	242	69xR	1m OGS
Jun07	243	28xR	1m OGS
Jun11	246	1xR	0.8m IAC80
Jun12	248	1xI,1xV	2.5 NOT
Jun14	249	1xV,1xR	0.8m IAC80
Jun24	260	1xR	0.8m IAC80
		18xR	1m OGS
Jun25	261	17xR	1m OGS
Jun28	264	17xR	1m OGS
Jul01	267	1xV,1xR	0.8m IAC80
Jul02	268	2xR	1.52 Loiano
Jul03	269	1xR	1.52 Loiano
Jul04	270	1xV,1xR	0.8m IAC80
Jul05	271	336xB	2.5 NOT
Jul06	272	1xV,1xR	0.8m IAC80
		887xB	2.5 NOT
Jul11	277	1xV,1xR	0.8m IAC80
Jul14	280	1xV,1xR	0.8m IAC80
Jul15	281	1xV,18xR	0.8m IAC80
Jul16	282	1xR	1m JKT
Jul17	283	1xR	0.8m IAC80
Jul19	285	1xR	0.8m IAC80
Jul20	286	1xR	1m JKT
Jul21	287	1xR	0.8m IAC80
		1xR	1.52 Loiano
Jul22	288	1xR	0.8m IAC80
Jul23	289	1xR	1.52 Loiano
Jul24	290	1xR	1.52 Loiano
Jul27	293	1xR	1.52 Loiano
Jul30	296	168xR	1m OGS
Jul31	297	59xR	1m OGS
Aug05	302	1xR	0.8m IAC80
Aug06	303	1xR	0.8m IAC80
		1xR	1.52 Loiano
Aug07	304	1xR	1.52 Loiano
Aug08	305	1xV,1xR	0.8m IAC80
Aug09	306	1xV,1xR	0.8m IAC80
Aug10	307	1xR	1.52 Loiano
Aug11	308	1xR	1.52 Loiano
Aug18	315	1xR	1.52 Loiano
Aug19	316	1xR	1.52 Loiano
Aug20	317	1xR	1.52 Loiano
Aug21	318	1xR	1.52 Loiano
Aug24	321	1xR	0.8m IAC80
Aug25	322	1xR	0.8m IAC80
Aug27	324	1xR	0.8m IAC80
Aug28	325	1xR	0.8m IAC80
Aug29	326	1xR	0.8m IAC80
Aug04	332	1xR	0.8m IAC80
Aug05	333	1xR	0.8m IAC80
Sep27	355	6xR	4.2m WHT
Sep28	356	16xR	4.2m WHT
Oct17	374	1xV	2.5m NOT
Nov04	393	6xR	2.5m INT
Nov05	394	5xR	2.5m INT

\*HJD–2451460

**Table 2.** Log of spectroscopic observations

Date	HJD(*)	Number of spectra	Telescope
99 Oct28	20	1	1.52m G.D. Cassini
99 Oct28	20	7	2.5m INT
99 Oct29	21	24	2.5m INT
00 Jul11	277	12	4.5m WHT

\*HJD–2451460

**Figure 1.** *R* band 1800 s image of XTE J1859+226. The field of view is 1.4 x 1.0 arcmin. XTE J1859+226 is indicated by an arrow and the contaminating star by the letter C. The magnitudes of stars 1–5 are listed in Table 3

on the Intermediate Dispersion Spectrograph (IDS) (range 3500–5000 Å, spectral resolution 1.02 Å/pixel). The exposure times ranged from 300–600 s for individual spectra. A single 2400 s spectrum was obtained with the 152cm G.D. Cassini Telescope at Loiano Observatory using BFOSC. The slit width was 2.5" and the spectral range 3500–9000 Å. The second series of spectroscopic observations were carried out on July 11 2001, during the second optical minioutburst described in section 4. We observed XTE J1859+226 using the ISIS spectrograph on the 4.2m WHT in Observatorio del Roque de los Muchachos, using typical exposure times of 1800 s. Standard IRAF procedures were used to de-bias the images and to remove the small scale CCD sensitivity variations. One dimensional spectra were then extracted from the processed images using the optimal extraction method (Horne 1986). Wavelength calibration was interpolated between contemporaneous exposures of a copper–argon arc lamp. No flux calibration was performed on the spectra, instead continuum normalization was applied.

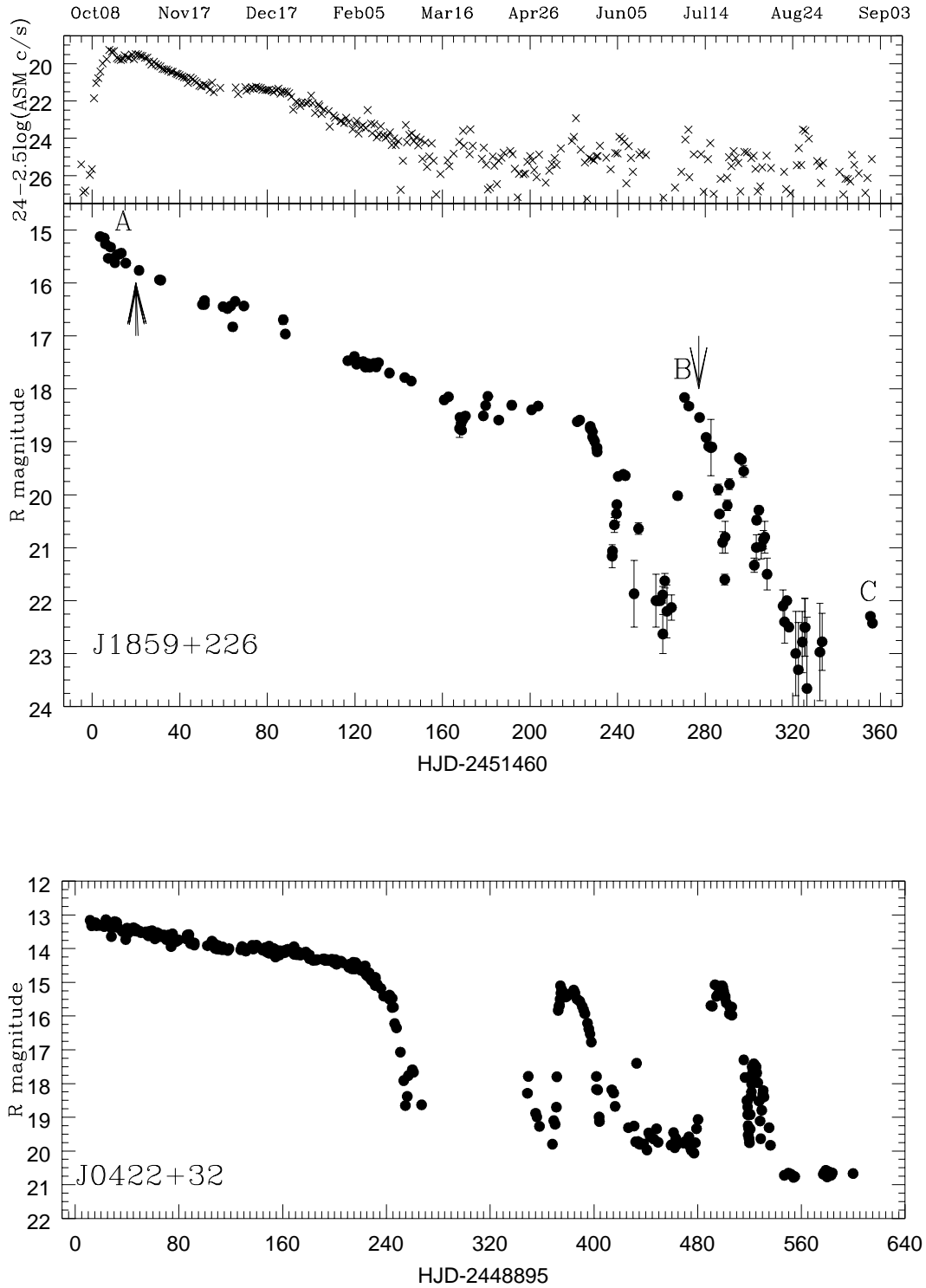


**Figure 2.** **Top:** Temporal evolution of J1859+226 plotted as 'X-ray magnitudes' [ $24-2.5\log(\text{XTE}/\text{ASM Count Rate})$ ] and *R*-band magnitudes averaged for each day. Note that 1 Crab equals an XTE/ASM count rate of 75 counts/sec. A, B and C mark the epochs studied for photometric and spectrometric variability. The arrows indicate the dates when spectra were taken. **Bottom:** *R* band light curve of XTE J0422+32 plotted for comparison. The J0422+32 data were provided by E. Kuulkers.

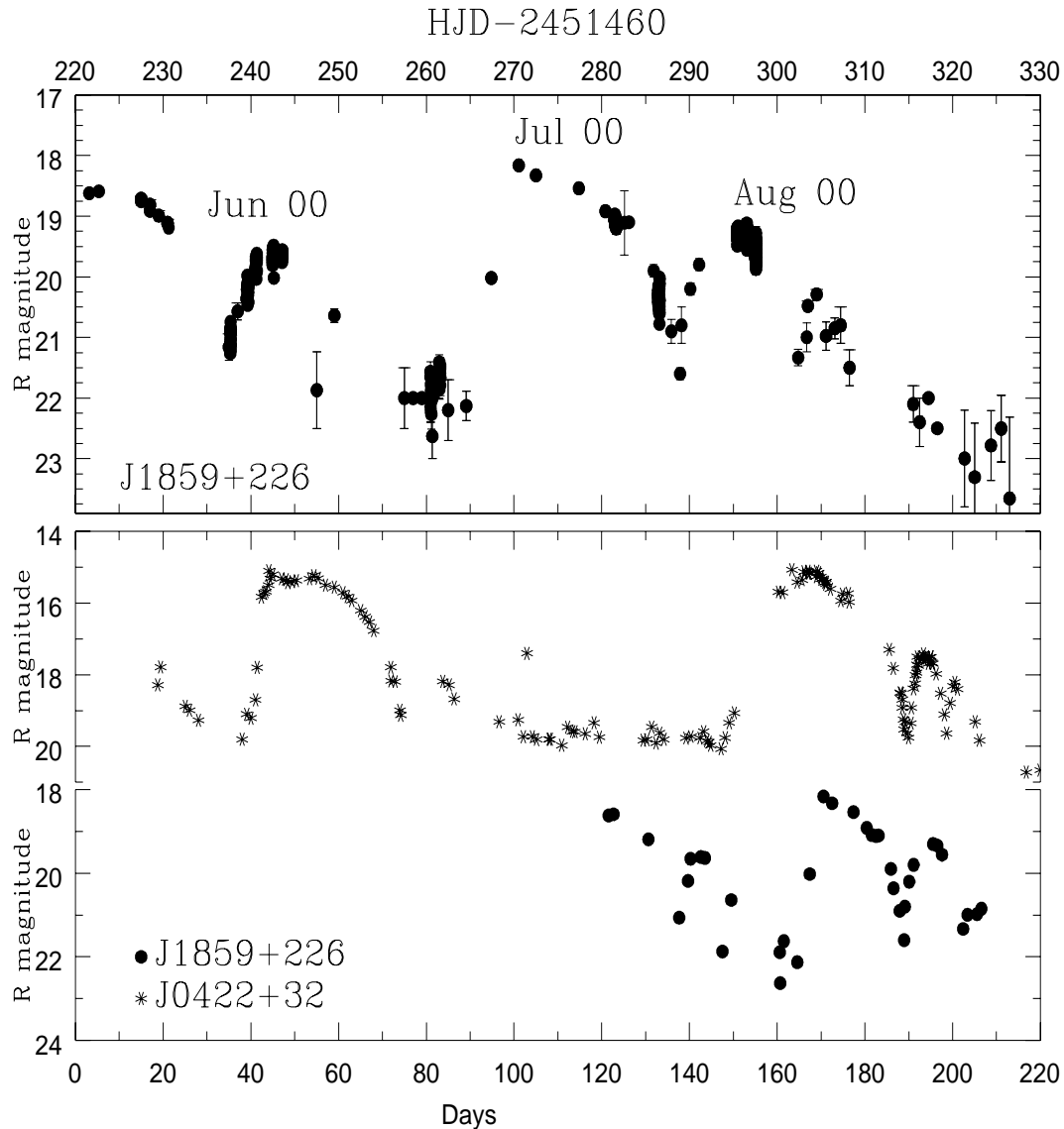


**Figure 3. Top:** The decline of the main outburst of J1859+226 showing the subsequent minioutbursts. The three minioutbursts are marked as Jun 00, Jul 00 and Aug 00. **Bottom:** The minioutburst of J0422+32 plotted for comparison (asterisks). We have superimposed the J1859+226 minioutbursts on the same scale (filled circles). For both systems, the last point marks the day when quiescence is reached. The J0422+32 data were provided by E. Kuulkers.

**Table 3.**  $R$  magnitudes for the contaminating star and 5 faint comparison in the field of J1859+226

$C$	1	2	3	4	5
23.05	20.31	19.41	18.86	20.15	19.58
$\pm 0.04$	$\pm 0.06$	$\pm 0.05$	$\pm 0.05$	$\pm 0.06$	$\pm 0.05$

### 3 LONG TERM BEHAVIOUR

Both the X-ray and optical properties of XTE J1859+226 were very similar to those of previously well-studied black hole SXTs, and so we embarked on a campaign of systematic monitoring of the decay light curve. Optical outburst light curves of SXTs tend to be fragmentary and generally cover only the main outburst. We note that the only SXT that

has been extensively covered throughout the entire outburst and subsequent decay activity is GRO J0422+32 (Callanan et al. 1995, Chevalier & Ilovaisky 1995). Figure 2 therefore compares the overall 1-yr light curve of GRO J0422+32 with that of XTE J1859+226 in optical ( $R$ -band) and X-rays (2–12 keV), since the X-ray turn-on of 9 October 1999. The basic properties of the outburst light-curve, are summarized in Table 4. They are similar to the light curves reported in Chen et al. 1997. The optical light curve can be classified as *FRED*: ‘fast-rise exponential-decay’, characterized by a smooth decline of 0.017 mag/day. At about the time that the X-rays dropped below the RXTE sensitivity limit, the optical light curve began a precipitous fall from  $R \sim 18.5$  to  $R \sim 22.5$  (day 210 after outburst). About 12 days after the peak of the outburst, the X-ray intensity reaches a secondary maximum which is not visible in our optical data.

**Table 4.** Basic properties of the outburst.

<i>Date of the outburst:</i>	Oct.1999
<i>X-ray light curve</i>	
<i>Morphology type:</i>	FRED
<i>Instrument and E band:</i>	ASM(RXTE)/2–12 KeV
<i>Flux at the peak:</i>	0.25 Crab
<i>Rise timescale (<math>\tau_r</math>):</i>	2.5 days
<i>Decay timescale (<math>\tau_d</math>):</i>	34 days
<i>Duration of the rising phase (<math>T_r</math>):</i>	13 days
<i>Duration of the decay phase (<math>T_d</math>):</i>	155 days
<i>Optical light curve</i>	
<i>Morphology type:</i>	Exponential decay No rise phase data
<i>Peak magnitude</i>	R=15.1, V=15.3 mags
<i>Quiescent magnitude</i>	R=22.48, V=23.29 mags
<i>Outburst amplitude (<math>m_{quiet}-m_{peak}</math>)</i>	$\Delta R=8.4, \Delta V=7.8$ mags
<i>Decay timescale (<math>\tau_d</math>):</i>	103 days
<i>Duration of the decay phase (<math>T_d</math>):</i>	220 days

A 'glitch' of  $\Delta R \sim 0.5$  mag was detected in the exponential decay phase, at about Mar 25 ( $\sim 165$  days after the peak), and in the X-ray light curve about 5 days earlier ( $\sim 160$  days from the outburst). Similar glitches have also been observed in the optical light curve of A0620-00 (Tsunemi et al. 1977), with a magnitude increase of  $\Delta B \sim 0.5$  mag about 150 days after the onset of the outburst, and also in J0422+32 with  $\Delta V \sim 0.3$  mag (Callanan et al. 1995). In X-rays, glitches are seen in the light curves of J0422+32, A0620-00, 1543-47, and 1124-683 (Chen et al. 1997).

Shortly after this rapid decline began, we have detected 3 minioutbursts or small amplitude (relative to the primary peak) events superposed on a 'normal' decay profile, when XTE J1859-226 was approaching quiescence (see Figure. 3). The first one (Jun 00) occurs  $\sim 240$  days after the peak, has an amplitude of 1.3 mag in *R* (with respect to the base level of Jun 2000) and lasts for  $\sim 20$  days. After the minioutburst, the decay follows roughly the same decline as before. The second minioutburst (Jul 00) occurs  $\sim 265$  days after the peak, reaches a maximum of  $R \sim 18$  ( $\Delta R \sim 4.7$  mag) and lasts for  $\sim 25$  days. And the third (Aug 00) reaches a peak only  $\sim 2$  mags above the previous minimum. The source then decays linearly to  $R \sim 23$  about 30 days after the onset on this last event. Minioutbursts have only been previously detected in GRO J0422+32 (Chevalier & Ilovaisky 1995) and GRS 1009-45 (Bailyn 1992) but this may be a consequence of inadequate monitoring (or lack of sensitivity) once the outburst is over. In J0422+32, two principal minioutbursts were observed (see Figure.2). Both had an amplitude of  $\Delta V \sim 5$  mag and lasted for  $\sim 20-40$  days. Here the minioutbursts reached the same level as the extrapolated light curve before the precipitous fall and are followed by events of smaller amplitude, as occur in J1859+226 Jul 00 minioutburst. Despite these similarities, the shape of the long term light curve in J0422+32 is completely different. Here the rate of decay in the *R*-band is only 0.0056 mag/day, which is a remarkably slow rate (Callanan et al. 1995). We note that both the duration of the main outburst and the minioutbursts is approximately the same.

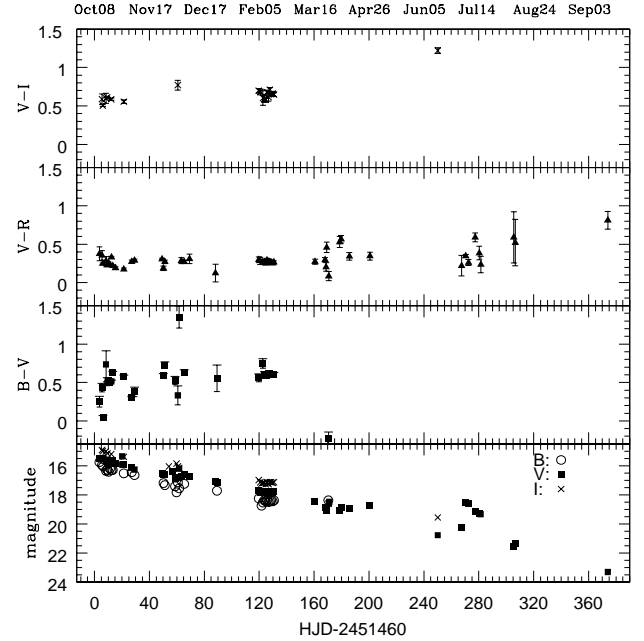
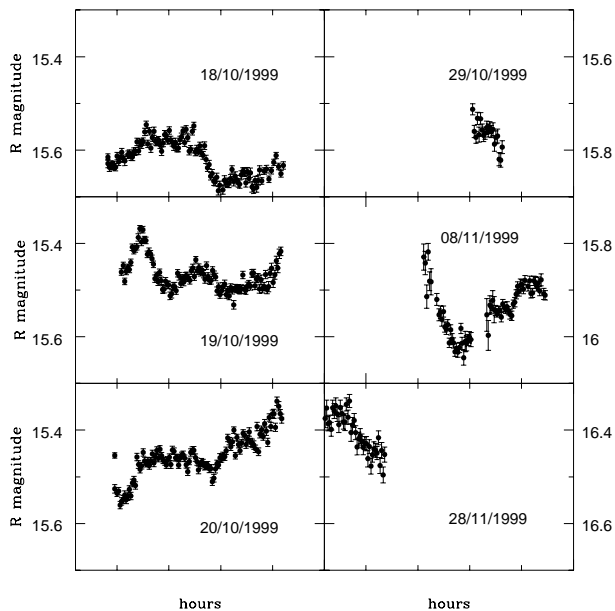
**Figure 4.** Long term variations of the  $V - I$ ,  $V - R$  and  $B - V$  colour indices of J1859+226 are plotted here against the overall light curve (bottom).

Figure 4 presents colour information of J1859+226 as a function of time. The mean  $V - R$  colour during outburst was measured to be  $\sim 0.27$  and remains constant during the main outburst. The source does not show detectable colour changes during any given night. It is clear that the system reddens as the system approaches quiescence and the secondary's contribution increases. During quiescence  $V - R = 0.81 \pm 0.11$ , which is consistent with the colour of a G9-K5 main sequence star.

From 24 Aug the system has reached quiescence with a mean magnitude of  $R = 22.48 \pm 0.07$  and  $V = 23.29 \pm 0.09$  (measured on 17 Oct). This yields a total amplitude for the optical outburst of  $\Delta V = 7.8$  mag, comparable to that observed for other SXTs (Chen et al. 1997).

#### 4 ANALYSIS OF PHOTOMETRIC VARIABILITY

Photometric variability has been explored in our best sampled data set. This includes a group of 6 nights at the peak of outburst (18–20, 29 October 1999, 8 and 28 November 1999), 2 nights during the maximum of the July minioutburst (5–6 July 2000) and 4 nights in quiescence (27–28 September 2000 and 4–5 November 2000). Hereafter, we will refer to data taken during the main outburst, the Jul 00 minioutburst and quiescence as Epochs A, B and C respectively and they are marked in Figure. 2.



**Figure 5.** Optical light curves for XTE J1859+226 on different nights in Epoch A. Note the remarkable changes in the light curve shape during each night.

#### 4.1 Epoch A: Irregular Variability

Representative light curves of XTE J1859+226, at the beginning of the outburst, are presented in Figure 5. We note the remarkable changes in shape and amplitude with no evidence for repeatability. Intermittent modulations of this type during decline from outburst on timescales at or near the orbital period have been seen in GS 2000+25 (Charles et al. 1991), Nova Muscae 1991 (Bailyn 1992) and Nova Persei 1992 (Callanan et al. 1995; Chevalier and Ilovaisky 1994).

Fourier analysis of these October data, shows three main peaks of comparable significance at 0.1600, 0.1907 and 0.2353 days in the power spectrum. However, no clear modulation is obtained after folding the data on these periods. We also note that none of these periods have been observed by other authors. For example periods of 0.2806 days (Uemura et al. 1999) and 0.3813 days (Garnavich et al. 1999) were reported during the first phase of the outburst. Nonetheless, the determination of orbital periods of X-ray novae during outburst has proved notoriously unreliable, e.g. modulation in the outburst light curve at a period much shorter than the orbital period has been seen in V404 Cyg (i.e. Wagner et al. 1990, Gotthelf et al. 1991). On the other hand it has been suggested that J1859+226, has a binary period shorter than 1 day, since the dereddened optical spectral energy distribution of J1859+226 during outburst can be represented by a steep blue power law flattening in the ultraviolet, and this resembles energy distributions of other short-period SXTs (Hynes et al. 1999).

#### 4.2 Epoch B: 22 min QPOs

High time resolution (30 to 60 s) *B*-band light curves were obtained on 5 and 6 July when J1859+226 was at the maximum of a minioutburst (see Figure. 6). The light curve on Jul 5 shows an extended 'dip' of about 0.3 mag lasting for 3 hr. During this dip, the source exhibited remarkable *QPO* flaring activity with  $\sim 20$  per cent amplitude. On July 6, the *QPO*s has disappeared and instead the source exhibited a smooth sinusoidal modulation with  $\sim 0.10$  mag amplitude. Studying the rapid variability seen on July 5, we find a period of  $21.7 \pm 0.6$  min using a periodogram analysis. This *QPO* timescale is very close to that reported by Hynes et al. 1999. The flaring ceased when the source returned to its predip level.

A periodicity of 0.78 days has also been reported from contemporary data (McClintock et al. 2000), which is claimed to be the orbital period. Their light curve shows evidence for a deep primary minimum (interpreted as the eclipse of the disc by the companion star) and a shallow secondary minimum. Assuming that the 0.3 mag dip in the July 05 light curve is the primary minimum, it occurs at HJD 2451731.51, which is exactly 1.3 days before McClintock's et al. primary minimum. Therefore the true orbital period would be a submultiple of 1.3 days, which automatically rules out the 0.78 d period (Zurita et al. 2000).

#### 4.3 Epoch C: Quiescent ellipsoidal modulation

Data taken in quiescence during 2000 September 27 and 28, on the 4.2 m WHT, and 2000 November 4 and 5 on the 2.5 m INT, exhibit a sinusoidal modulation, with a peak-to-peak amplitude of about 0.4 mag. We applied a Chi-squared minimization method in order to characterize the periodicity present in the data. Periodogram is shown in Figure 7. The periodogram shows several peaks although formally the peak with the highest significance is found at  $0.1594 \pm 0.003$  days. Assuming that this is actually a double-humped ellipsoidal light curve, as is typical of quiescent soft X-ray transients, the orbital period would then be  $0.3188 \pm 0.003$  days ( $\sim 7.7$  hours). We note that this period is roughly a submultiple of 1.3 days. This suggests that the variability (and in particular the 0.35 mag drop observed in the July minioutburst), might be related to the orbital period. However, periods from 0.14 to 0.23 days ( $P_{orb} \sim 6.6$  to 11.2 hrs) are equally possible at the 68 percent confidence level. Clearly more and higher quality data are needed to determine conclusively which period is the true orbital period.

We note that Filippenko & Chornock (2001) report a  $9.16 \pm 0.08$  hr ( $0.382 \pm 0.03$  days) modulation in the radial velocities of only 10 spectra, spread over two nights, obtained during quiescence. This period is consistent with our data and previous reports by Garnavich et al. (2001) and Sánchez-Fernández et al. (2000). Since all the dataset are affected by aliasing, it is clear that more spectroscopic/photometric observations are required to determine the true orbital period.

In Figure 8 we show the quiescent data folded on the 0.319 days period (top panel) and on the  $0.382 \pm 0.03$  days Filippenko's spectroscopic period (bottom panel). By com-

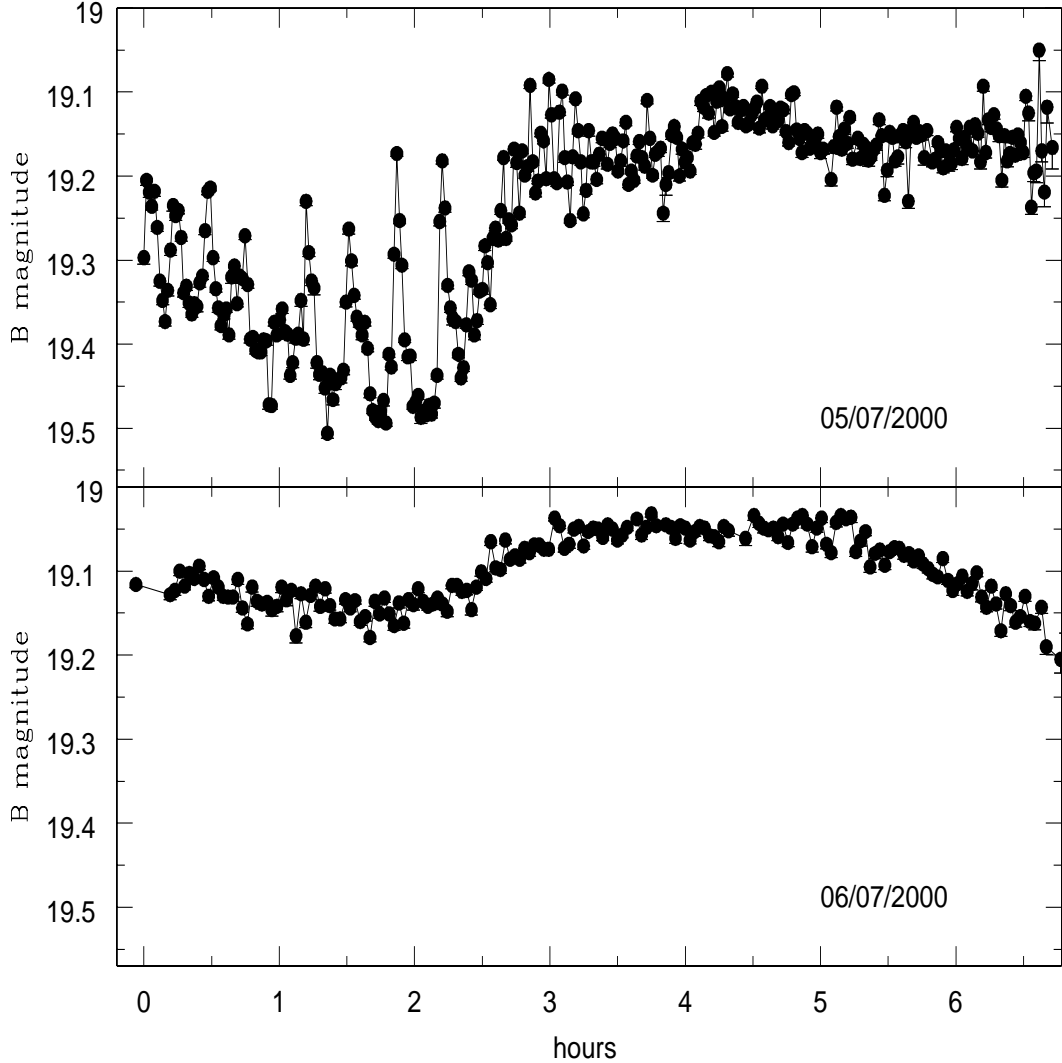


**Figure 6.** B-band light during Epoch B (Jul00 minioutbursts) of J1859+226 on 5 (top) and 6 Jul (bottom). The data points have been obtained with the 2.5m NOT. Note the flares in the Jul 5 light curve.

paring the amplitude of the curve with other SXTs in quiescence, we conclude that the the binary inclination must be high. The different depths in the minima also support this idea since this is only evident when the inclination angle is high.

An alternative way to estimate the orbital period is through the  $V$  amplitude of the outburst light curve ( $\Delta V$ ), by the use of the empirical relation

$$\Delta V = 14.36 - 7.6 \log P_{orb}(hr)$$

(Shahbaz & Kuulkers 1998). Taking  $V(\text{peak})=15.5$  and  $V(\text{quiescence})=23.3$ , we obtain  $P_{orb} \sim 7.30$  hr (0.30 days) which is consistent with the previous values.

## 5 ANALYSIS OF SPECTRAL VARIABILITY

Spectral variability has been explored in epoch A (Oct.20–28) and in the epoch B minioutburst (Jul.11). Days when spectra were taken are marked by arrows in Figure. 2 and are plotted in Figure. 9.

### 5.1 Epoch A

The bluer spectrum displayed typical emission lines of X-ray transients in outburst: He II 4686 Å, the Bowen blend at 4630–4640 Å and 3097–4103 Å, and Balmer emission from H $\beta$  to H $\delta$ . The H $\beta$  emission line is embedded in a broad absorption, as is often observed in the Balmer emission lines from SXTs (e.g. Casares et al. 1995). The main interstellar features were the CaII interstellar bands at 3933.66 and 3968.47 Å, (probably with some contribution from H $\epsilon$  absorption at 3970 Å), and the diffuse interstellar band at 4430 Å.

The only prominent feature in the redder spectrum is H $\alpha$  emission. The main interstellar features were the blend at 5778, 5780 and 5797 Å, the blend due to the interstellar Na I D lines at 5889 and 5895 Å, and the interstellar band at 6280 Å. The HeII and Balmer lines appear to be double peaked with separations of 300–500 km s $^{-1}$ , notably smaller than those detected in the outburst spectra of GRO J0432+22 (Callanan et al. 1995) or in the quiescent spectra of Nova Muscae 1991 or A0620-00 (Orosz et al. 1994). Dou-



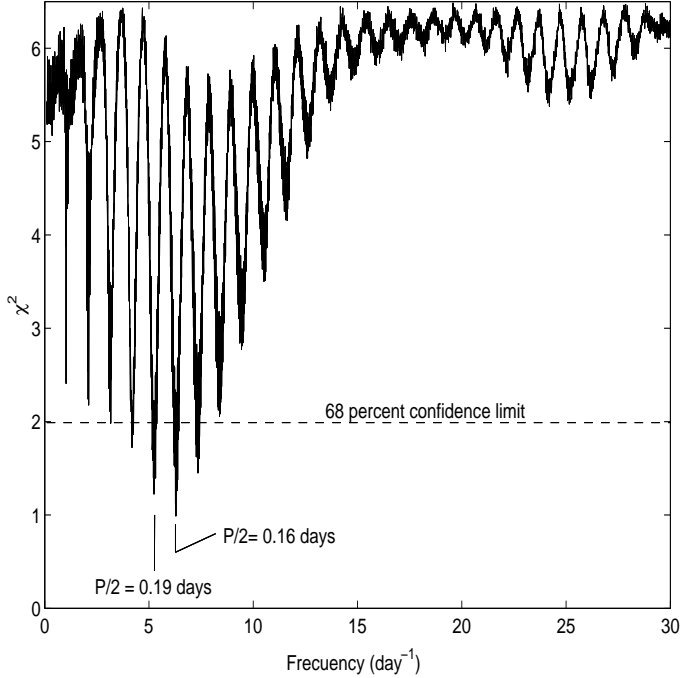


**Figure 7.**  $\chi^2$  minimization spectrum of the quiescent data. The deepest minima are marked, corresponding to  $P_{orb} \sim 0.32$  and  $P_{orb} \sim 0.38$  days.

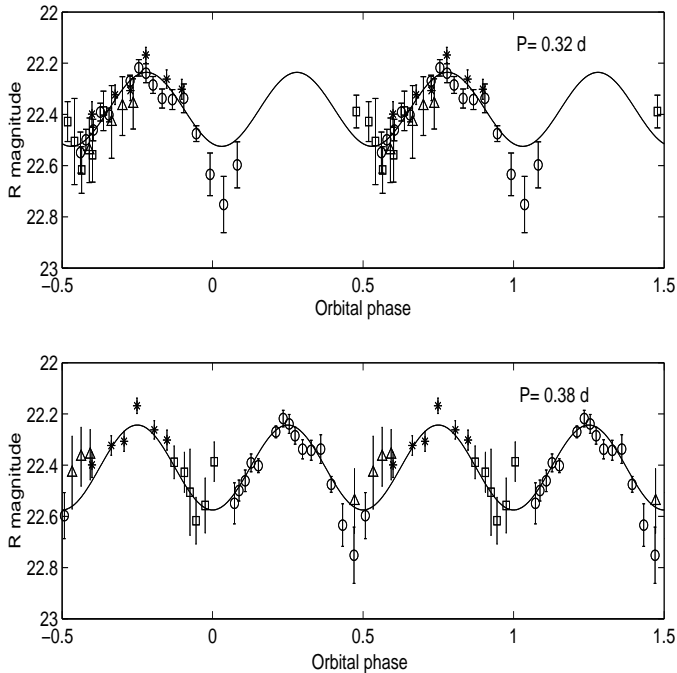


**Figure 8.** Optical photometry of XTE J1859+226 during the quiescent state (Epoch C) folded on the 0.319 d period (top panel) and on the 0.382 d period found by Filippenko & Chornock (bottom panel) and a superimposed sinusoidal fits. We have represented points taken on different days/sites with different symbols: asterisks (27/09/2000 – WHT), circles (28/09/2000 – WHT), squares (04/11/2000 – INT) and triangles (05/11/2000 – INT).

ble peaks were not detected in the Bowen blend lines in our spectra, most probably due to the blending phenomena than to the absence of such structure. However, the Bowen blend could also arise from other emitting region in the system.

## 5.2 Epoch B

The second series of spectra of the source were obtained on July 11 2000, near the maximum of that minioutburst. The bluer spectra displayed prominent Balmer emission from  $H\beta$  to  $H9$ . Bowen emission was not detected in these observations. On the other hand,  $CII$  emission at  $4267 \text{ \AA}$  was present. The main interstellar features were again the interstellar absorption at  $3968 \text{ \AA}$ , which affects the  $H\epsilon$  emission line, the diffuse  $CaII$  bands and the diffuse interstellar band at  $4430 \text{ \AA}$ . The Balmer lines also appear to be double peaked in minioutburst, with typical separations of  $500\text{--}700 \text{ km s}^{-1}$ , notably larger than the separations observed during main outburst. The red spectra display  $H\alpha$  emission and  $HeI$  emission lines at  $5877$  and  $6680 \text{ \AA}$ . The  $He I$  line at  $5877$  is affected by the interstellar blend of the  $Na I D$ . The interstellar bands at  $\sim 5780 \text{ \AA}$  and  $6280 \text{ \AA}$  are also detected.

The only observations of previous minioutburst spectra of SXTs are those from GRO J0422+32 (Casares et al. 1995; Callanan et al. 1995) and GRS 1009–45 (Bailyn & Orosz 1995). The spectra from GRO J0422+32 showed broad shallow  $H\beta$  absorption, and  $H\alpha$  evolving from absorption to emission on a timescale of 3 days. The spectra from GRS 1009–45 showed weak  $H\alpha$  and weak  $H\beta$  absorption. In none of them evidence of  $He I$  is found. Casares et al. 1995 also obtained phase resolved  $H\alpha$  and  $H\beta$  spectra of J0422+32 during its 1993 minioutburst. Balmer lines were embedded in broad absorptions whereas  $HeII$  was purely in emission and showed evidence of a large amplitude ( $\sim 755 \text{ km s}^{-1}$ ) S-wave component.

### 5.2.1 Variability of the emission lines

To examine the variability of the emission lines during the minioutburst, the equivalent widths were measured in the individual spectra as a function of 0.319 d period (see Figure. 10). The equivalent widths of the lines were measured after normalization of each individual spectrum by its continuum so that the variations in the lines are separated from variations in the continuum. Unfortunately, this study was not possible with the main outburst data, due to the poor S/N ratio of the individual spectra. Sinusoidal fits have been included in the plots as a reference. We can see that the  $H\alpha$  equivalent width is dependent on orbital phase. The same relation is less clear in  $H\beta$ , probably due to the smaller amplitude of the variations, but it is still present. The variation in the equivalent widths for both of them can be roughly reproduced with a sinusoidal function equal to the orbital period of the system, thus pointing to the changing visibility of a region of enhanced emission or bright spot, perhaps the splash point where the gas stream and accretion disc meet. Unfortunately, the uncertainty in our  $T_0$  prevents to define the absolute phasing in the EW curves. No clear modulation is seen in the EWs of  $H\epsilon$  and  $HeII$  which have means of  $5.95 \pm 0.95 \text{ \AA}$  and  $5.41 \pm 1.40 \text{ \AA}$  respectively.

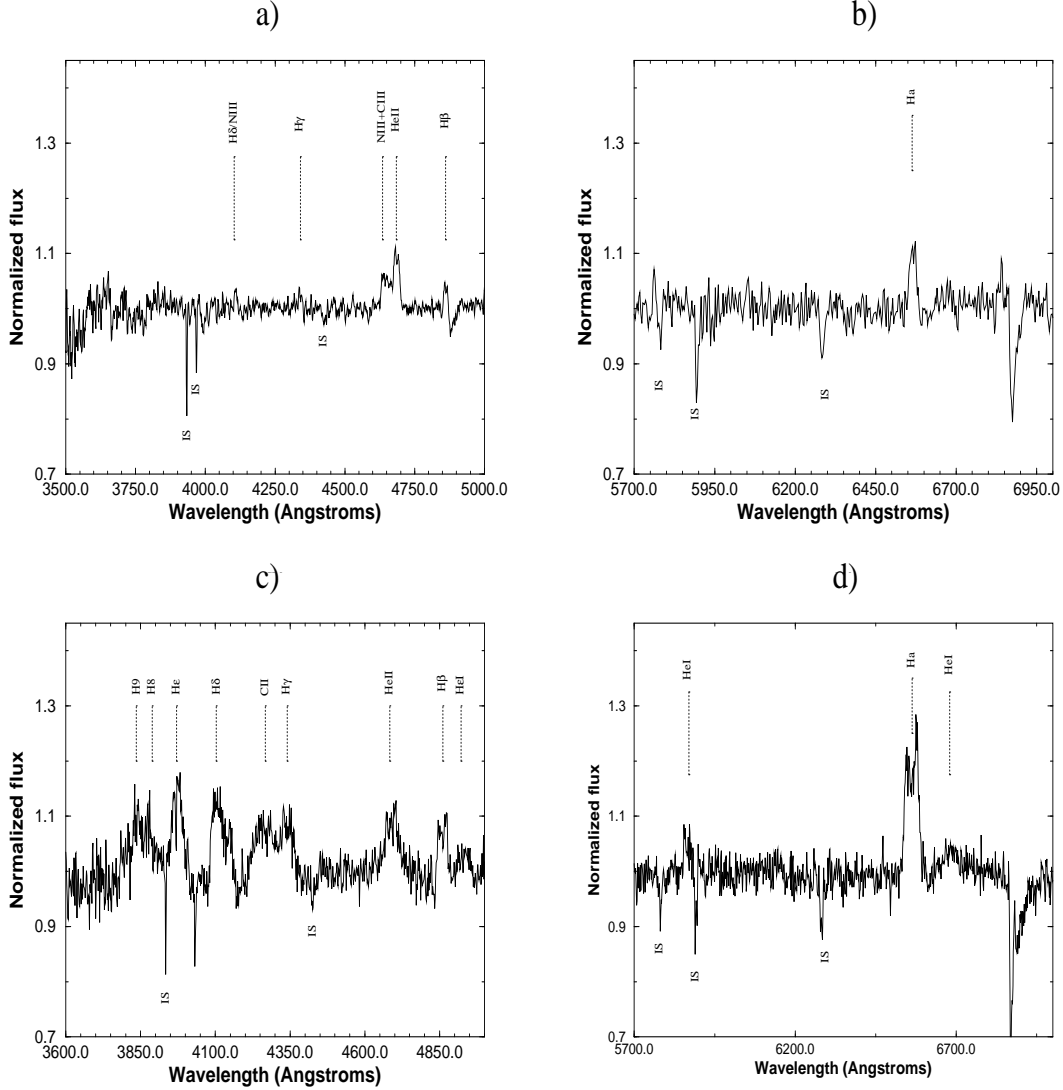


**Figure 9.** Spectroscopic observations of XTE J1859+226 during Epoch A (main outburst)– figures a and b– and during Epoch B (July 00 minioutburst)–figures c and d.

## 6 DISCUSSION

### 6.1 Distance estimate

In the context of King & Ritter’s model ( 1998), the exponential decay of the X–ray light curve indicates that irradiation is strong enough to ionize the entire accretion disc. Also, a secondary maximum is expected one irradiated-state viscous time after the onset of the outburst and this can be used to calibrate the peak X–ray luminosity and hence the distance to the source  $d_{\text{kpc}}$  through

$$d_{\text{kpc}} = 4.3 \times 10^{-5} t_s^{3/2} \eta^{1/2} f^{1/2} F_p^{-1/2} \tau_d^{-1/2}$$

where  $F_p$  is the peak X–ray flux,  $t_s$  the time of the secondary maximum after the peak of the outburst in days,  $\tau_d$  the e–folding time of the decay in days,  $\eta$  the radiation efficiency parameter and  $f$  the ratio of the disc mass at the start of the outburst to the maximum possible mass (Shahbaz et al. 1998). In our case,  $\tau_d=34$  d,  $t_s \simeq 68$  d and  $F_p$  can be esti-

mated from the XTE count rate (250 mCrab in the energy range 2–10 keV) which corresponds to  $1.7 \times 10^{-8}$  erg cm $^{-2}$  s $^{-1}$ . Assuming  $\eta=0.15$  and  $f=0.8$  we find  $d_{\text{kpc}} = 11$ .

Alternatively, we can estimate the distance to the source by comparing the quiescent magnitude with the absolute magnitude of a main sequence star which fits within the Roche lobe of a 7.65 hr orbit. Combining Paczynski’s (1971) expression for the averaged radius of a Roche lobe with Kepler’s Third Law we obtain the well-known relationship between the secondary’s mean density and the orbital period:  $\bar{\rho} = 110/P_{\text{hr}}^2$  (g cm $^{-3}$ ). Substituting for the orbital period of J1859+226 we obtain  $\bar{\rho}=1.87$  g cm $^{-3}$  which corresponds to a K0V–K1V secondary star with absolute magnitude  $M_R \simeq 6.1$ . The dereddened quiescent magnitude is  $V=23.27$  (using  $A_V=1.80 \pm 0.07$  as derived from the NaID line; see Hynes et al. 1999) which yields  $d_{\text{kpc}} = 11$ . This value perfectly agrees with that obtained previously, although strictly

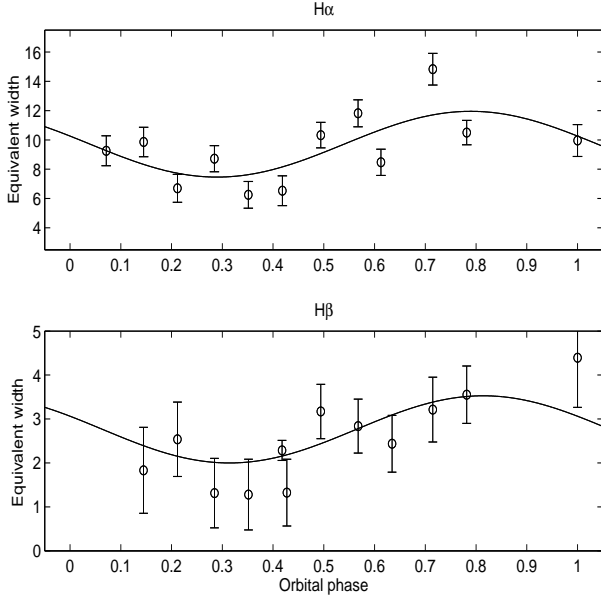


**Figure 10.** Equivalent width variations for H $\alpha$  and H $\beta$ , during Epoch B (Jul00 minioutburst).

speaking, this is a lower limit to the distance as we are neglecting any contribution by the accretion disc to the quiescent optical flux. Although the measured (V–R) color is consistent with the calculated density, a spectral type determination of the companion star is essential to refine this distance estimate.

### 6.2 Relative contribution of the disc

Following the color evolution of the system, we can compute the relative contribution of the disc to the optical flux in the V and R bands as a function of the assumed spectral type of the companion star. Assuming that the colour of the secondary star corresponds to a normal dwarf of a fixed spectral type and that the colour of the disc remains constant during the main outburst (as we can see in Figure 4), then we can relate the fluxes of the disc and star in the R and V bands:  $f_{V_{disc}} = h \times f_{R_{disc}}$ ,  $f_{V_{star}} = k \times f_{R_{star}}$ , where  $h \propto 10^{(V-R)_{disc}}$  and  $k \propto 10^{(V-R)_{star}}$ . It is straightforward to calculate the relative contribution of the disc ( $f_{V_{disc}}/f_V$  and  $f_{R_{disc}}/f_R$ ) through:

$$f_V = h \times f_R + (k - h) \times f_{R_{star}}$$

where  $f_V$  and  $f_R$  are the measured fluxes in the V and R bands. The unreddened colours (V–R) corresponding to spectral types G5V to M0V are taken from Schmidt–Kaler (1982). We also assume  $E(B-V)=0.58$  from Hynes et al. 1999. The results are shown in Table 5.

During the first phase of the outburst, the optical emission is almost completely dominated by the accretion disc. The relative contribution of the disc reaches a minimum when the system drops to the faint level between the June 00 and July 00 minioutbursts.

**Table 5.** Relative contribution of the disc in the R and V band (bold), assuming different spectral types for the companion star.

HJD(*)	G5V	K0V	K5V	M0V
10	0.99	0.99	0.99	0.99
	<b>1.00</b>	<b>1.00</b>	<b>1.00</b>	<b>1.00</b>
21	0.99	0.99	0.99	0.99
	<b>1.00</b>	<b>1.00</b>	<b>1.00</b>	<b>1.00</b>
65	0.99	0.99	0.99	0.99
	<b>1.00</b>	<b>1.00</b>	<b>1.00</b>	<b>1.00</b>
120	0.96	0.97	0.98	0.98
	<b>0.99</b>	<b>1.00</b>	<b>1.00</b>	<b>1.00</b>
130	0.97	0.97	0.98	0.98
	<b>0.98</b>	<b>0.98</b>	<b>0.99</b>	<b>0.99</b>
160	0.93	0.94	0.95	0.96
	<b>0.95</b>	<b>0.95</b>	<b>0.97</b>	<b>0.98</b>
167	0.91	0.92	0.94	0.94
	<b>0.95</b>	<b>0.96</b>	<b>0.98</b>	<b>0.98</b>
200	0.92	0.92	0.94	0.95
	<b>0.93</b>	<b>0.94</b>	<b>0.96</b>	<b>0.97</b>
249	0.37	0.44	0.55	0.61
	<b>0.38</b>	<b>0.45</b>	<b>0.56</b>	<b>0.62</b>
267	0.64	0.68	0.73	0.76
	<b>0.63</b>	<b>0.66</b>	<b>0.75</b>	<b>0.78</b>
272	0.93	0.93	0.94	0.95
	<b>0.93</b>	<b>0.94</b>	<b>0.95</b>	<b>0.96</b>
281	0.85	0.86	0.89	0.91
	<b>0.84</b>	<b>0.85</b>	<b>0.88</b>	<b>0.90</b>

\*HJD–2451460

### 6.3 Properties of the disc

Using the same technique, we have fitted the unreddened B, V and R band fluxes to estimate the intrinsic colours of the disc. As we might expect, the fluxes during outburst are strongly correlated. We obtain  $(B-V)_{disc} \sim -0.07$  and  $(V-R)_{disc} \sim -0.10$ . These colours agree well with irradiated model predictions, where most of the reprocessed energy is radiated in the UV (see e.g. van Paradijs & McClintock 1995).

The ratio of outburst X-ray to optical luminosity [ $\xi = B_0 + 2.5 \log F_x(\mu\text{Jy})$ ] agrees with the observed distribution for LMXBs. Taking  $B=15.9$  (Chaty et al. 2000) and  $F_x(2 - 12\text{keV}) \simeq 250$  mCrab (Wood et al. 1999) at the outburst peak and assuming  $A_B=2.39$  (Hynes et al. 1999) we obtain  $\xi=20.9 \pm 0.4$ , whereas the distribution peak of LMXBs gives  $\xi=21.8 \pm 1$  (see van Paradijs & McClintock 1995). The moderately low  $\xi$  probably indicates a high binary inclination since the X-ray source in J1859+226 could be partially hidden by the accretion disc. This result is consistent with the evidence for two X-ray dips during the second outburst ( $\sim$ July 8) reported by Tomsick et al. 2000, and with the large amplitude (0.4 mag) of the quiescent ellipsoidal modulation.

### 6.4 The outburst mechanism

It is largely accepted that optical emission in SXTs outburst is due to irradiation of the outer disc by X-rays. Within this context, the optical emission must be correlated with the X-rays. However, we see features which have no correspondence between the X-rays and optical, such as a secondary

maximum  $\sim 12$  days after the peak of the X-rays outburst which is not visible in the optical band, and minioutbursts which are absent in the X-ray lightcurve. Such differences can not be explained in the context of a simple irradiated disc and an additional mechanism is necessary to explain them. Systems with clear discrepancies between X-rays and optical are J1655-40 (Esin et al. 2000) and J1550-564 (Jain et al. 2000). Both sources exhibit an exponentially declining optical light curve, whereas the X-ray remains constant or increases slightly. To explain the outburst light curves in these systems it has been suggested the classical dwarf-nova type instability followed by an episode of enhanced mass transfer from the secondary or up scatter of the optical flux into the X-ray by the corona. Our photometric colors indicate that the optical emission is dominated by X-ray reprocessing on the disc although in J1859+226 clearly interplay with viscous heating and geometrical effects (such as disc height variations and shadowing effects) are playing an important role in the differences between the X-ray and optical lightcurves.

The only SXTs where minioutbursts have been detected are XTE J0422+32 and GRS 1009-45, although this property does not seem to be a peculiarity of these systems, but a selection effect, due to the difficulty in obtaining continuous monitoring from outburst to quiescence. The most promising mechanism to produce minioutbursts is the *X-ray echo model* (Augusteijn et al. 1993, Hameury et al. 2000), where they are interpreted as due to enhanced mass flow from the companion star on the outer disc which is responding, essentially linearly, to heating by X-rays from the primary. The process goes on continuously, triggered by echoing the initial X-ray outburst.

The spectra taken during the main outburst show an emission feature at  $\lambda\lambda 4540-4550\text{\AA}$  which is the *Bowen Blend*, but it is not present in the Jul 00 minioutburst. This behavior has also been observed in J0422+32 (Casares et al. 1995, Callanan et al. 1995). The Bowen blend is a combination of high excitation lines (mainly CIII, OII and NIII at  $\lambda\lambda 4634-4642$ ), produced by the fluorescence resonance mechanism which initially requires seed photons of HeII Ly $\alpha$  at  $\lambda 303.78$ . Under the hypothesis that the composition of the accreting material has not changed substantially since the onset of outburst, the absence of Bowen emission in the minioutburst spectra must be ultimately related to the weakness of the X-ray photoionizing continuum which originates the whole cascade process. We do not have enough information in our data to make detailed calculations of this process. However, it seems that the reprocessed X-rays make a small contribution to the optical flux during minioutburst: in an irradiated disc, the average ratio of X-ray to optical luminosity yields  $L_X(2-11\text{ keV})/L_{opt}(300-700\text{ nm}) \simeq 500$ . We can estimate this rate during the highest minioutbursts (Jul 00). Tomsick et al. 2000 report a  $3.11 \times 10^{-11}\text{ erg cm}^{-2}\text{ s}^{-1}$  flux near the maximum of the minioutburst in the range 2.5-20 keV, which was well above the expected quiescent X-ray flux level. Assuming the energy spectrum is described by a power law with a photon index 2.03 as they reported, we can estimate the flux in the range 2-11 keV. Taking a  $B$  magnitude of  $B \sim 19.2$ , the estimated X-ray to optical ratio is  $L_X(2-11\text{ keV})/L_{opt}(300-700\text{ nm}) \sim 4$ . This means that the X-ray

spectrum during minioutburst must be much harder than during primary outburst or, alternatively, that the optical flux during minioutburst is instead dominated by the intrinsic luminosity of the disc. During the primary outburst, the intensity and width of the Balmer lines is notoriously smaller than in the minioutburst spectra as expected because the continuum is 2 mag brighter. The change in line size is probably reflecting a shrinking in disc size. Alternatively the emission line cores might be filled in with narrow emissions during the main outburst.

Another possibility could be that minioutbursts are produced by a temporal enhancement of viscosity in the quiescent disc just after the main outburst (Osaki et al. 1997). However, there is no easy explanation as to why the viscosity can vary in such a way.

## 7 ACKNOWLEDGMENTS

We thank G. Dalton for contributions to the observing campaign and E. Kuulker for providing the optical light curve of J0422+32. Part of this work is based on observations made with the European Space Agency OGS telescope operated on the island of Tenerife by the Instituto de Astrofísica de Canarias in the Spanish Observatorio del Teide of the Instituto de Astrofísica de Canarias. TS was supported by an EC Marie Curie Fellowship HP-MF-CT-199900297.

## REFERENCES

- Augusteijn T., Kuulkers E., Shaham J., 1993, *A&A*, 279, L13  
 Bailyn C.D., 1992, *ApJ*, 391, 298  
 Bailyn, C.D., Orosz J.A., 1995, *ApJ*, 440, L73  
 Callanan P.J., Garcia M.R., McClintock J.E., Zhao P., Remillard R.A., Bailyn C.D., Orosz J.A., Harmon B.A., Paciasas W.S., 1995, *ApJ*, 441, 786  
 Casares J., Martin A.C., Charles P.A., Martin E.L., Rebolo R. Harlaftis E.T., Castro-Tirado A.J., 1995, *MNRAS*, 276, L35  
 Charles P.A., Kidger M.R., Pavlenko, E.P., Prokof'eva, V.V., Callanan P.J., 1991, *MNRAS*, 249, 567  
 Charles, P. A., Hynes, R. I., Casares, J., Israelian, G., Rodriguez-Gil P., Shahbaz, T., Zurita, C., Abbott, T., Hakala, P., King, A.R., 2000, AAS High Energy Astrophysics Division  
 Chaty S., Haswell C.A., Norton A.J., Hynes R.I., Smail I., Solheim J., Ostensen R., Greve T.R., Fynbo J., Horne K., O'Brien K., Skidmore W., Fried R., Krisciunas K., Garnavich P.M., Garcia M., Contreras M., Harlaftis E.T., Charles P.A., Shahbaz T., Kuulkers E., Chen W., Shrader C.R., Howell S.B., Wagner M., 1999, *IAUC*, 7284  
 Chen W., Shrader C.R., Livio M., 1997, *ApJ*, 491, 312  
 Chevalier C., Ilovaisky S.A., 1995, *A&A*, 297, 103  
 Esin A.A., Lasota J.P., Hynes R.I., 2000, *A&A*, 354, 987  
 Filippenko A.V., Chornock R., 2001, *IAUC*, 7644  
 Garnavich P.M., Stanek K.Z., Berlind P., 1999, *IAUC*, 7276  
 Garnavich P., Quinn J., 2000, *IAUC*, 7388  
 Gotthelf, E., Patterson, J., Stover, R.J., 1991, *ApJ*, 374, 340  
 Hameury J., Lasota J., Warner B., 2000, *A&A*, 353, 244  
 Horne K., 1986, *PASP*, 98, 609  
 Hynes R.I., Haswell C.A., Norton, A.J., Chaty S., Solheim J.E., Ostensen R., Abbott T.M. C., Fried R., McFarland J., Rolfe D.J., Lott D.A., Ioannou Z., Shafter A., O'Brien K., Horne K., Krisciunas K., Ivison R.J., 1999, *IAUC*, 7294

- Jain R.K., Bailyn C.D., Orosz J.A., McClintock J.E., Sobczak G.J., Remillard R.A., 2000, *ApJ*, 546, 1086
- King A.R., Ritter H., 1998, *MNRAS*, 293, L42
- Landolt A.U., 1999, *ApJ*, 104, 340
- McClintock J.E., Remillard R.A., Heindl W.A., Tomsick J.A., 2000, *IAUC*, 7466
- Orosz, J.A., Bailyn, C.D., Remillard, R.A., McClintock, J.E., Foltz, C.B., 1994, *ApJ*, 436, 848
- Osaki Y., Shimizu S., Tsugawa M., 1997, *PASP*, 49, L19
- Paczyński B., 1971, *Annual Review of Astronomy and Astrophysics*, 9, 183
- Sánchez-Fernández C., Zurita C., Casares J., Shahbaz T., Castro-Tirado A., 2000, *IAUC*, 7506
- Schmidt-Kaler, T.H., 1982, *Landolt-Bernstein New Series, Volume 2b, Astronomy and Astrophysics—Stars and Star Clusters*, eds. K. Schaifers, H.H. Voigt, Springer-Verlag, New York
- Shahbaz T., Kuulkers E., 1998, *MNRAS*, 295, L1
- Shahbaz T., Charles P.A., King A.R., 1998, *MNRAS*, 301, 382
- Stellingwerf, R.F., 1978, *ApJ*, 224, 953
- Stetson P.B., 1987, *PASP*, 99, 191
- Tomsick J.A., Heindl W.A., 2000, *IAUC*, 7456
- Tsunemi H., Matsuoka M., Takagishi K., 1977, *ApJ*, 211, L15
- Uemura M., Kato T., Pavlenko E., Shugarov S., Mitskevich M., 1999, *IAUC*, 7303
- van Paradijs J., McClintock J.E., 1995, *X-Ray Binaries*, Cambridge University Press, Cambridge
- Wagner R.M. et al., 1990, in *IAU Colloq. 122: Physics of Classical Nova*, p. 429
- Wagner R.M., Smith P.S., Schmidt G.D. Shrader C.R., 1999, *IAUC*, 7279
- Wood A., Smith D.A., Marshall F.E., Swank J., 1999, *IAUC*, 7274
- Zurita C., Casares J., Rodríguez-Gil P., Shahbaz T., Charles P.A., Sánchez-Fernández C., Castro-Tirado A., Abbot T., Hakala P., 2000, *Proceeding of the Granada Microcuasar Symposium*, Kluwer Academic Publishers